

NEW AND EFFICIENT NEUTRINO FACTORY FRONT-END DESIGN

Tuesday May 17, TPPP047

J.C. Gallardo, J.S. Berg, R.C. Fernow, H. Kirk, R.B. Palmer, BNL, Upton, NY 11973, USA
D. Neuffer, FNAL, Batavia, IL 60510, USA; K. Paul, Muons, Inc., Batavia, IL 60510, USA

This study was carried out under the rubric of the **Joint Study on the Future of Neutrino Physics: The Neutrino Matrix** organized by the APS Divisions, DPF, DNP, DAP, DPB.

The main objective of the study (ST2B) was to achieve a **cost-effective** Neutrino Factory in line with the realization in (FS2) that the front-end represented $\approx 40\%$ of the total facility costs and the acceleration RLAs accounted by $\approx 20\%$. The new design is driven by

- ❑ Optimization of the capture section
- ❑ Use of adiabatic rf phase rotation and bunching section
- ❑ Double the transverse acceptance of the accelerator chain following the cooling section
- ❑ Use of combination of RLA and FFAG rings in the acceleration section (see J.S. Berg *et al.*, MPPE017, MPPE026)

Consequences

- ➡ Bunching less expensive
- ➡ Cooling Section is simpler, shorter and significantly less expensive
- ➡ It is possible to transport both signs μ^+ and μ^- .

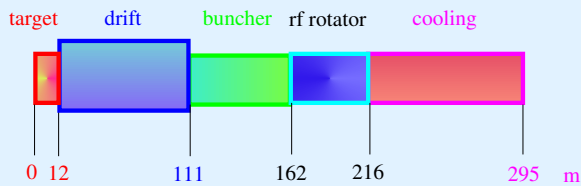


Figure 1: Layout of the ST2B Front-End.

Different Components of the Front-End

- * **Capture Section:** Hg jet target; AGS type proton beam. Solenoidal channel: Length ≈ 12 m, $20 \leq B_z \leq 1.75$ T
- * **Decay Drift:** Length ≈ 100 m, $B_z = 1.75$ T
- * **Adiabatic Bunching:** 27 cavities with 13 different \downarrow frequencies and changing \uparrow gradients. Length ≈ 50 m, $B_z = 1.75$ T

$$333 \leq f \leq 234 \text{ MHz} \quad 5 \leq \text{Grad.} \leq 10 \text{ MV/m}$$

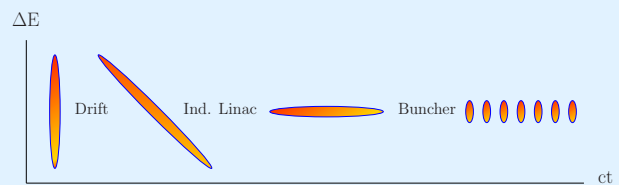
- * **Phase Rotator:** 72 cavities with 15 different \downarrow frequencies; constant gradient. Length ≈ 50 m, $B_z = 1.75$ T

$$232 \leq f \leq 201 \text{ MHz} \quad \text{Grad} = 12.5 \text{ MV/m}$$

- * **Cooling:** Solenoidal FOFO lattice; Length ≈ 80 m, $B_z = \pm 2.8$ T; Grad. = 15.25 MV/m, $f = 201.25$ MHz

Bunching and Phase Rotation Region

Study2 (FS2) with Induction Linacs



Neuffer's Bunched Beam Rotation with 201 MHz rf

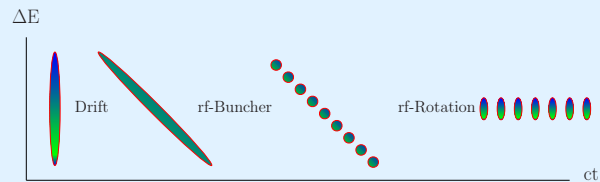


Figure 2: (Color) Comparison of the buncher concept used in ST2B (bottom) with the bunching system used in FS2 (top).

The longitudinal phase space after the target is the same in both cases. Initially, there is a small spread in time, but a very large spread in energy. The target is followed by a drift space in both cases, where a strong correlation develops between time and energy. The induction linacs was shown to reduce the final rms energy spread to 4.4%. The beam was then sent through a series of rf cavities for bunching, which increased the energy spread to $\approx 8\%$.

In the scheme presented here, the correlated beam is first adiabatically bunched using a series of rf cavities with decreasing frequencies and increasing gradients. The beam is then phase rotated with a second string of rf cavities with decreasing frequencies and constant gradient. The final rms energy spread in the new design is 10.5%.

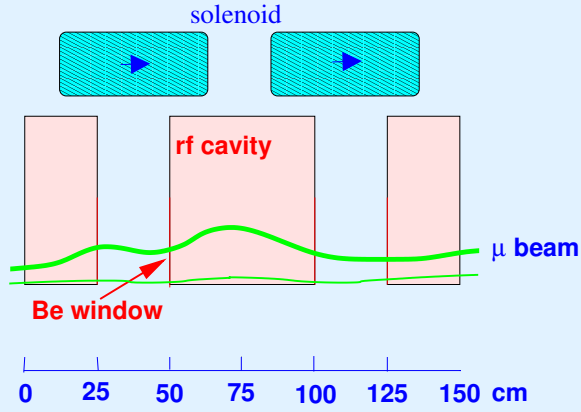


Figure 3: Schematic of 2 cells of the buncher or rotator section.

Cooling Section

A novel aspect of this design comes from using the windows on the rf cavity as the cooling absorbers. This is possible because the near constant β function does not significantly increase the emittance heating at the window location. The window consists of a 1 cm thickness of LiH with a $75\mu\text{m}$ layer of Be on the rf cavity field side and, $25\mu\text{m}$ layer of Be on the opposite side. (The Be will, in turn, have a thin coating of TiN to prevent multipactoring). The alternating 2.8 T solenoidal field is produced with one solenoid per half cell, located between the rf cavities.

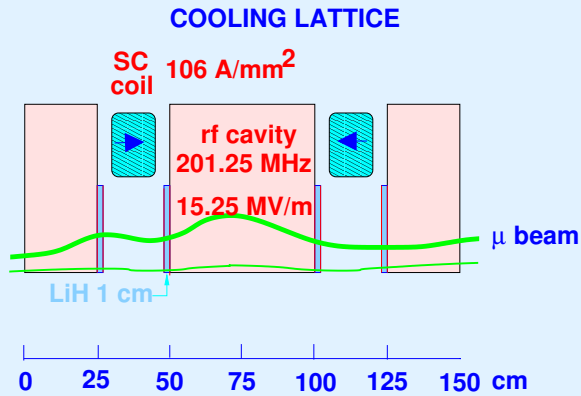


Figure 4: Schematic of one cell of the cooling section. Beta function is constant ≈ 80 cm. Windows are absorbers.

Simulation Performance

subsubsection30 T Solenoid on Target

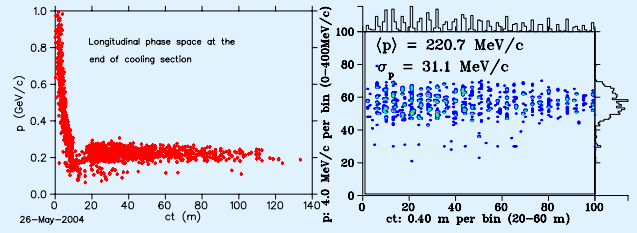


Figure 5: Longitudinal phase space at the end of the channel.

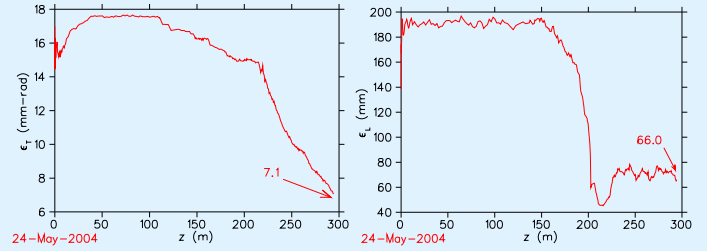


Figure 6: Normalized transverse emittance (left) and longitudinal emittance (right) along the front-end for a momentum cut $0.1 \leq p \leq 0.3 \text{ GeV/c}$.

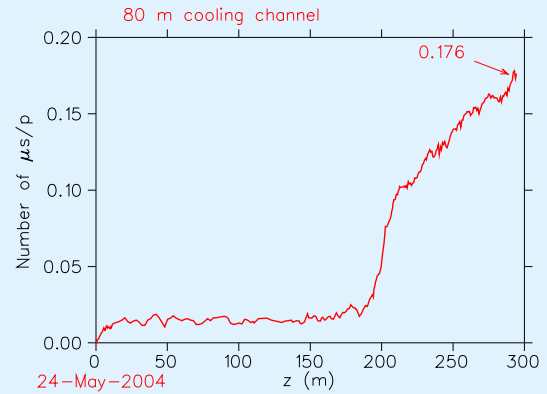


Figure 7: No. μ/p in A_{\perp} and A_L .

Table 1: Table of Results.

$\langle p_z \rangle$ Mean Momentum (MeV/c)	220
rms Energy Spread (MeV)	31
ϵ_{\perp}^N (mm-rad)	7.1
$\epsilon_{\perp}^{equil.}$ (mm-rad)	5.5
ϵ_L^N (mm)	66
A_{\perp} (mm-rad)	30
A_L (mm)	150
No. μ/p in A_{\perp} and A_L	0.170

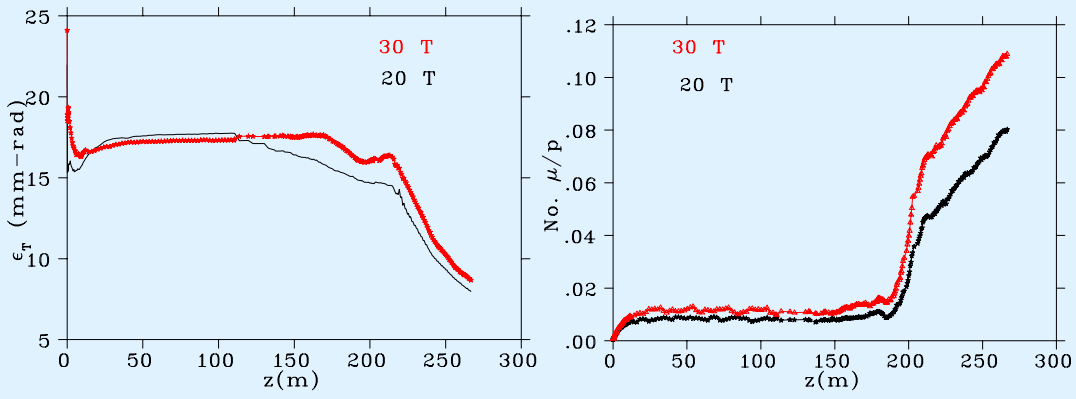


Figure 8: Comparison between 20 and 30 T examples: (left) transverse emittance vs z ; (right) number of muons per incident proton on target vs z .

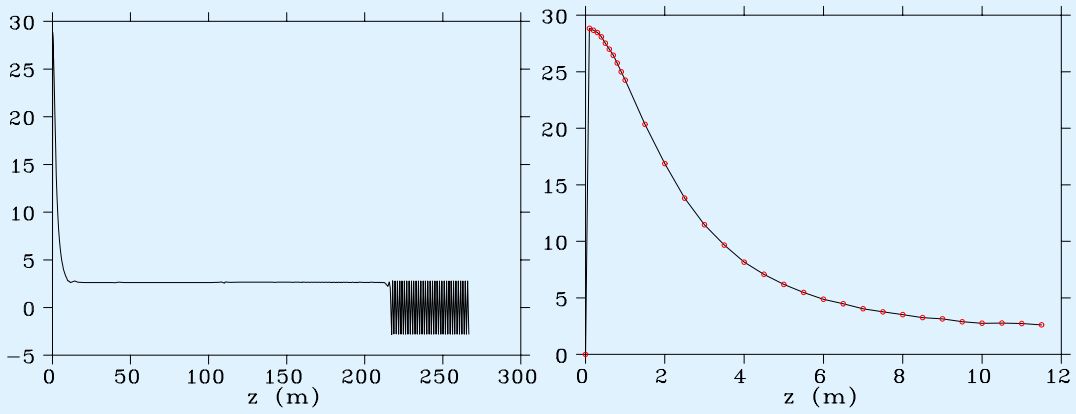


Figure 9: Magnetic field (left) on the total length of the front end; magnetic field (right) on the target region.

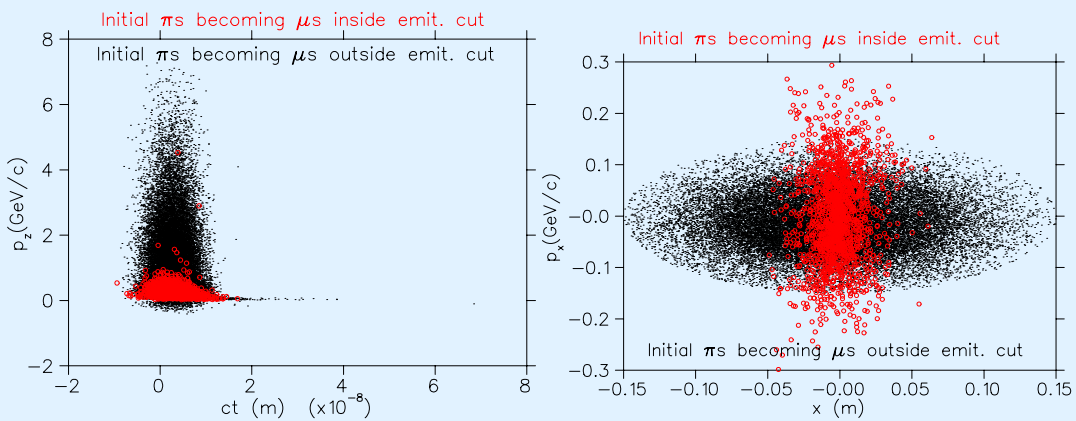


Figure 10: Longitudinal phase space (left); transverse phase space (right) of initial pions.